# Influence of regional stress field on vent alignment in monogenetic volcanic fields

Jordan Croll (jcroll@terpmail.umd.edu)

30 November 2020

Advisors: Dr. Laurent Montesi, Dr. Jacob Richardson

Department of Geology, University of Maryland College Park, MD 20742



### **Abstract**

How does lithospheric stress affect the distribution of volcanoes in a volcanic field? I hypothesize that the dominant alignment of vents in a Monogenetic Volcanic Field will be approximately parallel to the most compressive stress direction of the regional stress field. Magma transport in a Monogenetic Volcanic Field involves dikes and magmatic conduits that open from the dike and extend to the surface vertically and form volcanic vents. Dikes propagate as opening mode cracks in a direction parallel to the most compressive stress direction. For that reason, the spatial distribution of volcanic vents in a Monogenetic Volcanic Field may be influenced by the regional stress field, with the mean strikes of the lines linking vents approximately parallel to the most compressive stress direction. By representing the location of each vent in a monogenetic volcanic field as a point, the azimuths between them are calculated. A critical distance criterion is used to filter out insignificant vent pairs based on the assumption that vents with a large distance between them are likely independent. Data is available from the Newberry Volcanic Complex, the San Francisco Volcanic Field, the Springerville Volcanic Field, the Adams Volcanic Field, and the San Rafael Volcanic field. The mean azimuth between pairs of volcanoes in each field can be compared to the corresponding regional stress environment, obtained independently from the World Stress Map. A statistical test for the comparison between circular means called the V-test is used to quantify the agreement between the most compressive stress and the average vent pair azimuth. I found a strong preferred vent-to-vent azimuth, corresponding to the regional stress for the Newberry Volcanic Complex and the Adams Volcanic Field, which are associated with the Cascadia subduction zone. For large fields in an intraplate setting like the San Francisco Volcanic Field and the Springerville Volcanic Field, there is no well-defined preferred orientation of the azimuths within the field.

# 1 Background

#### 1.1 Monogenetic Volcanism

Most volcanoes on Earth and other terrestrial planets are basaltic in composition, monogenetic, meaning they usually only erupt once, and occur in fields called Monogenetic Volcanic Fields, or MVFs (Valentine and Conner, 2015). Most of the individual volcanoes, or vents, within an MVF are small in eruptive volume (typically less than 1 km<sup>3</sup>) but the number of vents in an MVF can range from one to over one thousand. Most MVFs contain tens to hundreds of vents. Basaltic MVFs occur in all tectonic settings, including subduction, rift, and intraplate activity. They can also form on the flanks or the surrounding areas of calderas, stratovolcanoes, or shield volcanoes. Although the MVF can be active for several million years, each vent has a geologically short life span, at most a few thousand years. For example, the Parícutin volcano, which famously erupted in a Mexican cornfield in 1943, is part of the Michoacán-Granajuato MVF. Parícutin erupted for only 9 years and is now considered inactive (Foshag and Gonzales, 1956; Luhr and

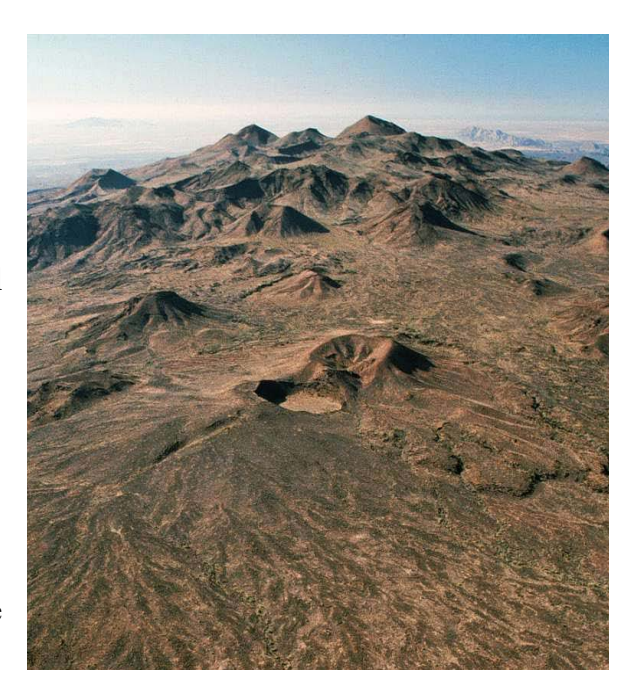


Figure 1

Vent cluster in the San Francisco Volcanic Field (Collier, 2010)

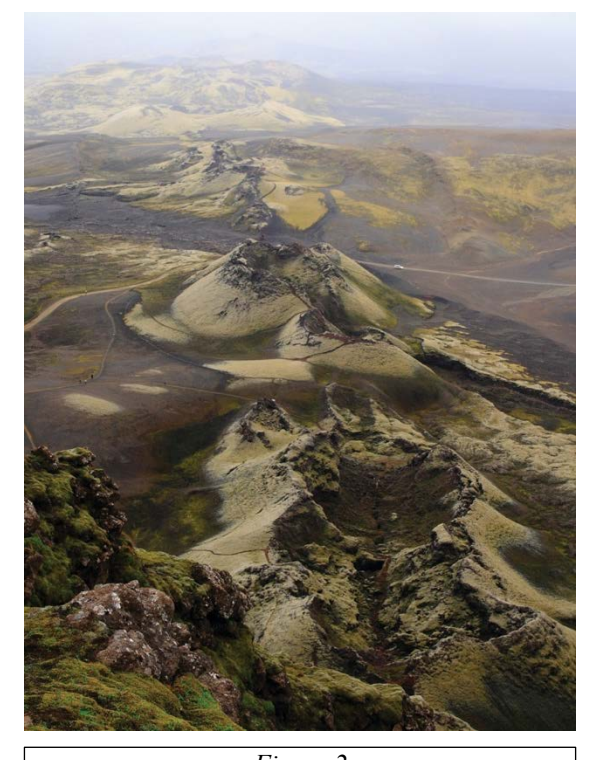
Simkin, 1993). Singular vents within a field can have different phases of magmatic and phreatomagmatic activity which makes interpretation of eruptive style more complex (Valentine and Conner, 2015).

Eruption styles between monogenetic and polygenetic volcanoes are generally similar in the way that eruptions are primarily driven by the expansion of volatiles (dominantly H<sub>2</sub>0, CO<sub>2</sub>, and sometimes SO<sub>2</sub>) that were previously dissolved in the magma. Whether the magma interacts with groundwater or surface water also influences the type of eruption and the resulting volcanic edifice. The most common style of volcano within an MVF is a scoria cone. Eruptions of scoria cones are produced mostly by their own internal volatiles (Valentine and Conner, 2015). Scoria cones are largely effusive but have a component of explosivity. Larger effusive magmatic eruptions can form small shield volcanoes within an MVF.

Phreatomagmatic eruptions take place in  $\sim 10\%$  of the volcanoes in an MVF but in certain fields greater than 50% of the volcanoes can be Phreatomagmatic generated. Phreatomagmatic eruptions occur when magma interacts with water near the surface and produces steam that releases upon eruption alongside other volatiles. This style of eruption is more explosive and generates maars, tuff rings, and tuff cones.

### 1.2 Effects of stress on magma ascent

Volcanic field distribution globally and on all terrestrial planets is influenced by regional tectonic environments (Valentine, 2008). A regional tectonic field changing over time can influence the location of volcanic field generation and the location of vent clusters within an individual field. There appear to be at least small vent distribution patterns within all volcanic fields (Valentine, 2008). As implied by the distribution of vents, vent clusters, and the general shape of the field, the regional tectonic setting influences the location of partial-melting in the mantle and magma transport through the mantle and crust (le Corvec, 2012).



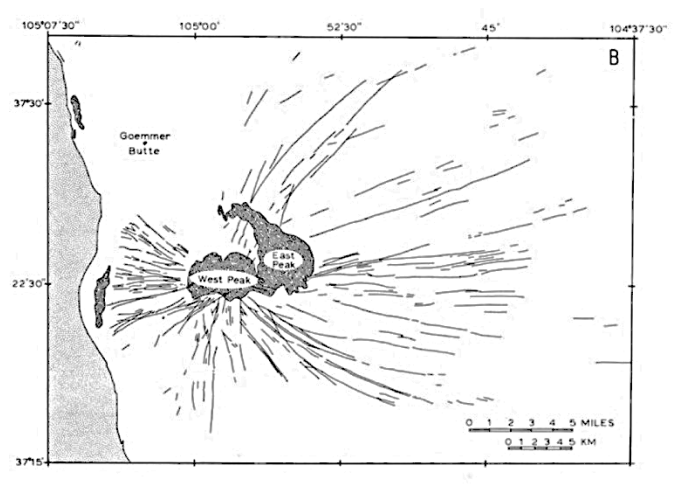


Figure 2

Conduits along a dike's path propagated to the surface and formed aligned vents at Laki Volcanic Fissure, Iceland

Britannica

Figure 3

The Spanish Peaks; Radial dike swarm reorients as the regional stress becomes the dominant stress field as the dikes propagate.

Johnson, 1968

Vent clusters of 10-100 vents are common in larger MVFs (e.g. Michoacan-Guanajuato, San Francisco MVFs) while clusters of 10-20 are common in smaller systems. Clustering can be explained by pre-existing magmatic plumbing systems or varying magma supply across the field (Valentine and Conner, 2015).

Alignments of volcanic vents within an MVF arise often (Valentine and Conner, 2015). Cinder cone morphology, magnetic data, and age-dating suggest azimuths with short length components between two vents arise over geologically short time scales (hundreds to thousands of years). In other words, volcanic vents nearby to one another usually erupt within thousands of years to one another. By studying and quantifying these alignments, the location and orientation of structures in the subsurface such as dikes can be inferred. For instance in Figure 2, at the Laki Volcanic Fissure in Iceland, conduits propagated from a dike to the surface to form aligned volcanoes. From the location of the vents at the surface, the location of a dike within the subsurface can be inferred.

Dike propagation is crucial for magma transport (Le Corvec et al., 2013). This fact naturally leads to the question of which direction dikes propagate toward. Dikes open in the direction of least compressive stress propagate perpendicular to that direction (Odé, 1957). Thus the stress regime plays a key role in determining the dike propagation direction (Le Corvec et al., 2013). Sediments at the Spanish Peaks dikes in the San Rafael Volcanic Field, Utah (Figure 3) have been eroded deeply enough that the ancient dike and conduit system is exposed at the present surface.

A map of the Spanish Peaks dike swarm in Figure 4 reveals how the dikes changed direction during propagation. Initially, the dikes extended radially from a central vent, principally under the influence of magma chamber pressurization. As they extended further from their origin, the regional stress field had more impact on their propagation. The dikes changed direction and reoriented themselves orthogonally to the least principal stress. Although dikes will often propagate in this way, there can be unexpected complications due to structures such as cracks or faults in the crust



Figure 4

San Rafael MVF; The dike and conduit system pictured here has been eroded over thousands of years of running water. This is important in understanding the connection between dike propagation and vent distribution.

Judy McIlrath

that can influence how a dike will propagate. A major assumption of this project is that dikes will propagate perpendicularly to the least principal stress.

Magma transport within an MVF is reliant on dikes and dike swarms (Valentine and Conner, 2015). Magma transport from dikes to the surface relies on magmatic conduits—usually cylindrical or near-cylindrical columns of magma shooting vertically off of dikes. The paths that the conduits take possibly take advantage of subsurface structures that intersect the dike and provide a complex plumbing system for magma to escape to the surface. This relation is evidenced by a strong statistical relationship between orientations of vent alignments and structural features in the subsurface such as cracks, faults, fractures, and joints (Valentine and Conner, 2015). Another proposed explanation for conduit propagation is pressure changes in the opening-mode crack that force the dike to bulge out to the most energy-efficient packing arrangement—for liquid, this is a cylinder. The cylindrical column then propagates to the surface and forms a volcano. Assuming that the formation of vents is linked to fractures in the crust, therefore, provides evidence that there exists a close relationship between vent distribution and the stress regime of the crust.

# 2 Field Information



JNIIED SIAIE

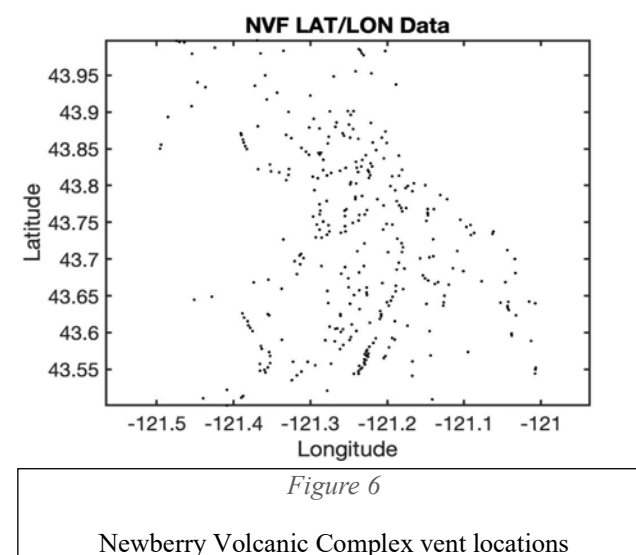
Figure 2

Locations of the MVFs studied in this paper. The Adams and Newberry Volcanic Fields are located near the Juan de Fuca subduction zone; The San Rafael, San Francisco, and Springerville Volcanic Fields are located on the Colorado Plateau.

Five MVFs in the Western United States have been analyzed in this study (Figure 5). The fields can be separated The Adams Volcanic Field and the Newberry Volcanic Complex are located in the Cascade Range near the Juan De Fuca Subduction Zone. The San Francisco Volcanic Field, Springerville Volcanic Field, and the San Rafael Volcanic Field are located within the Colorado Plateau where very little crustal deformation has affected its crust in the last 600 million years (Fillmore, 2011).

### 2.2 Newberry Volcanic Complex

The Newberry MVF is located on the Newberry Volcano, which also features a central caldera which is the largest volcano in the Cascade Volcanic Arc. The MVF consists mainly of more than 400 vents (Figure 6), mainly pyroclastic cones and lava domes around the caldera and the flanks of the volcano. No MVF in the contiguous United States has more vents (Donnelly-Nolan, 2011). The Newberry MVF has been active for about 600,000 years (Donnelly-Nolan, 2011) and the most recent eruption, which produced the "Big Obsidian Flow," took place about 1,300 years ago (Robinson et al., 2015). The field overlaps with the Northwest corner of the Basin and Range Province—this region is also



known as the High Lava Plains. Newberry is situated at the intersection of the Brothers Fault Zone with the north–northwest-trending Sisters and northeast-trending Walker Rim fault zones (Kienle and Wood, 1992). The overarching tectonic environment stems from the subduction of the Juan de

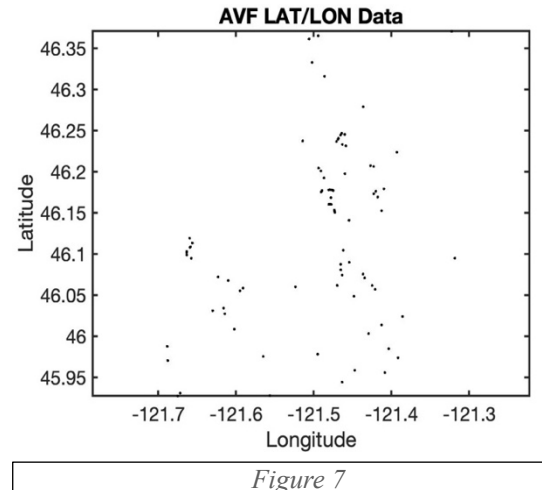
Fuca plate under the North American plate which is the driving factor of the cascade range.

#### 2.1 Adams Volcanic Field

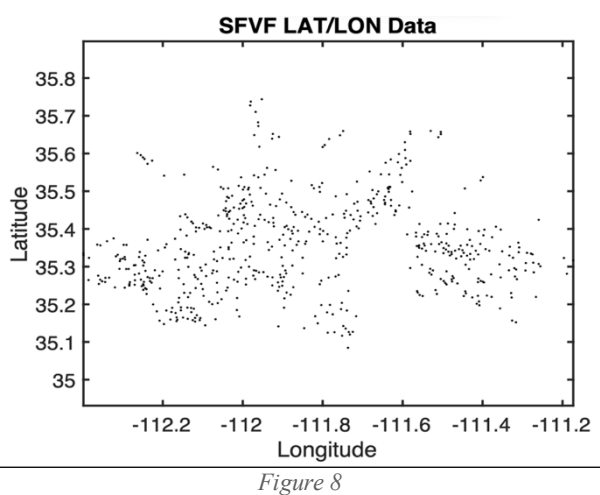
The Adams MVF is much like the Newberry MVF in the sense that it has a central vent and is located near a subduction zone. The central edifice, Mount Adams, is a large stratovolcano located in Southcentral to Southwest Washington state and part of the Cascade Range to the Southeast of Mt. Rainier. There are at least 120 vents in the MVF, most of which are andesitic cinder cones (Figure 7). Mount Adams' most recent eruption was approximately 1000 years ago, although the field itself is considered active and has been so for at least 1 Ma (USGS). Volcanism at Adams began around 940 ka, including three main eruptive stages occurring at ~500, ~450, and ~30 ka. The field is situated in the Cascade volcanic arc where volcanism is caused by the Juan de Fuca plate subducting under the North American Plate. This region of the Cascades is a hazard zone, especially the region between Mt. Rainier and Mount Adams.



Most volcanoes in the San Francisco Volcanic Field are basaltic cinder cones. More than 600 of the edifices (Figure 8) in the field are monogenetic and formed over months to years (USGS). The San Francisco Volcanic Field is situated atop the Colorado Plateau in an intraplate



Adams Volcanic Field vent locations



San Francisco MVF vent locations.

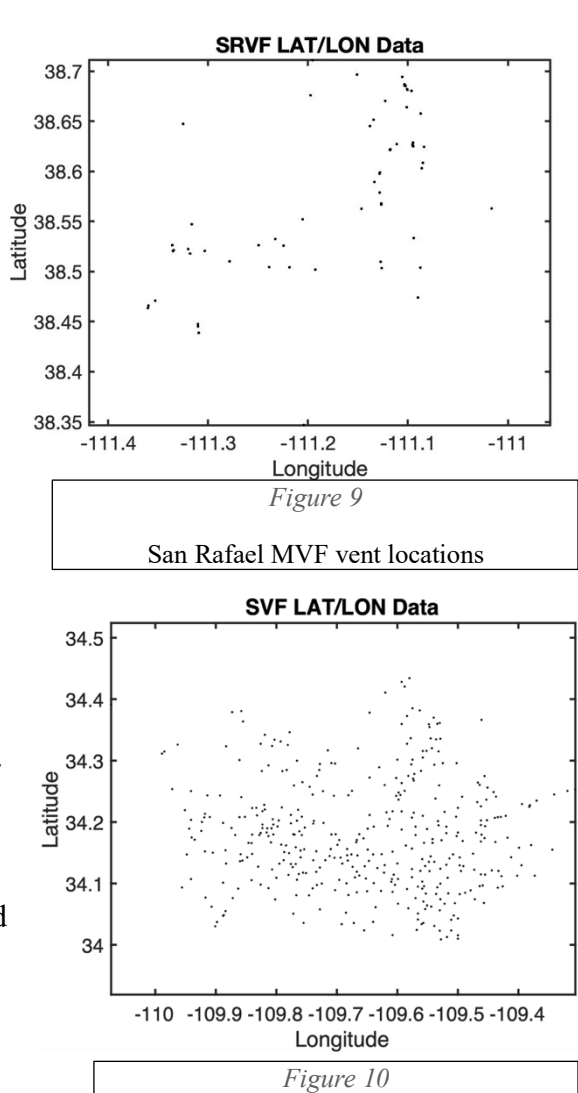
setting within the North American Plate near Flagstaff, AZ. Magma from the asthenosphere is able to rise into the lithosphere which provides the heat necessary for volcanism (USGS). The lack of a central vent at the San Francisco MVF leads to the scattered nature of the vents, with certain groupings of very dense vent distribution.

#### 2.4 San Rafael Volcanic Field

The San Rafael Swell is located in South-Central Utah about 14 miles from Green River, UT in an intraplate setting on the North American Plate. During the Laramide Orogeny, Precambrian dike swarms faulted and formed the San Rafael Swell. Those basement rocks below the Swell shifted upwards and formed an anticline with overlaying sedimentary material. Since its formation, thousands of years of hydrological erosion exposed the dikes, conduits, and older surrounding material to provide a snapshot of how the magma within the field distributed.

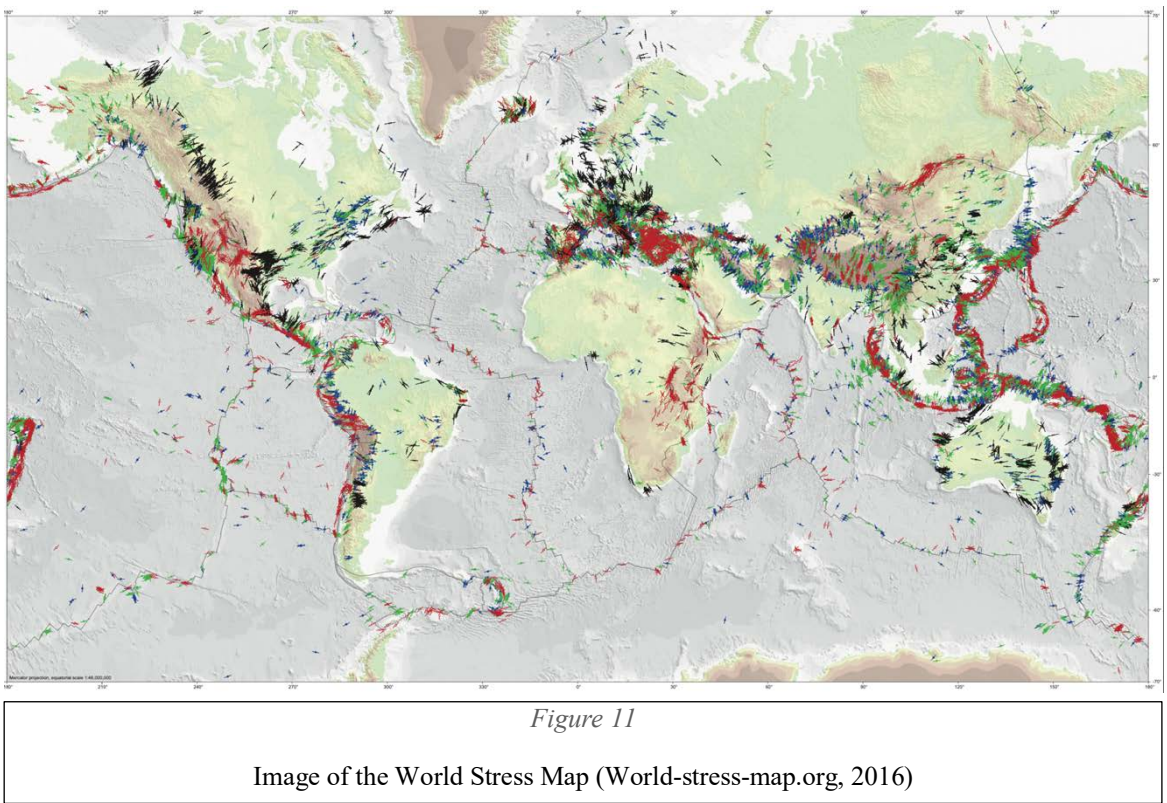
### 2.5 Springerville Volcanic Field

The Springerville Volcanic Field is located in East-Central Arizona on the Colorado Plateau. The field is Southeast of the San Francisco Volcanic Field and is located in an intraplate setting on the Colorado Plateau. The field consists of at least 405 distinct vents (Figure 9), most of which are basaltic cinder cones and monogenetic (Condit, 1996). This field also does not include a central vent which leads to a more distributed field much like San Francisco.



#### 3 Stress Data

To compare vent alignments to the regional stress, stress measurements that are independent of vent alignments are needed. I will be retrieving this data from the World Stress Map (Figure 11).



3.1 World Stress Map

The World Stress Map (WSM) will be the source of independent stress data used to compare against the vent alignments for each field. The map was conceived in 1986 as a project of the International Lithospheric Program and is maintained by the Helmholtz Centre Potsdam GFZ German Research Centre for Geosciences. The WSM is a collaborative project between academia and industry that aims to characterize the current crustal stress patterns and to understand the stress sources across the world. The map illustrates strikes in the direction of extension, lists the measurement technique, depth, latitude and longitude, and ratings of the measurement from A to E. Only measurements with quality grades A, B, or C are considered.

## 4 Methods

Determining whether the preferred orientation of alignments in an MVF will be parallel to the most compressive stress within the field involves three steps: 1) Identify the predominant alignment(s) of the field; 2) Determine the significance of those preferred orientations; and 3) Compare the distribution of those alignments to the relevant stress measurements from the WSM in a rigorous manner. I first used a dataset of randomly generated vent locations and determined the azimuths between them. These azimuths were then filtered by length such that only azimuths with a length component less than some critical distance,  $d_{crit}$  are kept. Then, the distribution of remaining azimuths was tested for uniformity. A random dataset should be uniform and have no significant mode. When working with real datasets that had a significant mode, the mean azimuth was compared to the most compressive stress direction from the WSM by using a circular V-Test in which a preordained mean value is compared to a circular distribution.

The mathematics required for analyzing angular data dispersed around a unit circle are not trivial and reside in the realm of circular statistics (Berens, 2009). To illustrate why cartesian

statistics will be ineffective, consider the following example. If two azimuths are within  $5^{\circ}$  of the N-S direction, one at  $5^{\circ}$  and another at  $175^{\circ}$ , it is intuitive that the mean angle should reside at  $0^{\circ}$ ; however, the average of  $5^{\circ}$  and  $175^{\circ}$  is  $90^{\circ}$ . Cartesian statistics would imply that the mean is  $90^{\circ}$  because these statistics are unaware of the correspondence between  $0^{\circ}$  and  $180^{\circ}$ .

The process for calculating the circular mean begins with converting the direction values into unit vectors as:

$$\boldsymbol{r}_i = \begin{pmatrix} \cos \alpha_i \\ \sin \alpha_i \end{pmatrix}$$

and then calculate the mean resultant vector defined as:

$$\bar{\boldsymbol{r}} = \frac{1}{N} \sum_{i} \boldsymbol{r}_{i}$$

Following this calculation, the four-quadrant arctangent function (in MATLAB, atan2) can be used to return the mean resultant vector to angular form, that is, as the angle (Berens, 2009).

A further complication arises as azimuth data are diametrically bimodal (Landler et al., 2018), that is, an azimuth of 5° is the same as 185° as there is no directionality in the line joining two vents. To remedy this issue, the angles used in this analysis are  $\alpha_i = 2A_i$ , and similarly, the mean orientation of the azimuth between the selected vent pairs is  $\bar{A} = \bar{\alpha}/2$  (Landler, 2018). Plotting the mean azimuth and the least principal stress together provides a rapid evaluation of the hypothesis that the two strikes are perpendicular to one another is reasonable.

### 4.1 Alignment Analysis

Two random one-dimensional arrays of size N were generated, one corresponding to longitude (X) and one corresponding to latitude (Y). These arrays are plotted in a scatter plot with MATLAB's scatter function. The geodesic distance  $D_m$  and azimuths  $A_m$  between all possible pairs of points are then calculated, using MATLAB's distance function, which conducts appropriate calculations assuming the points are at the surface of the Earth. The results are two  $N \times N$  matrices for  $D_m$  and  $A_m$ . Note that the diagonals of either matrix are zero since these values correspond to an azimuth drawn between identical endpoints. Each pair of points appear twice, as both the "forward-azimuth" and the "back-azimuth". Therefore, we reorganize the upper triangle of the distance matrix is reorganized as a vector using the *squareform* MATLAB function.

The goal of the alignment analysis is to measure the lengths and orientations of lines connecting all possible pairs of points (Cebriá et al., 2011). If there is a preferred strike of the connecting lines, there will be statistical evidence of a predominant orientation. The most general method of calculating azimuths in the field begins by calculating all azimuths. Attempting to extract a predominant alignment from every possible azimuth in the field may return a significant value, but likely will reflect the shape of the field (Wadge and Cross, 1988). A general all-neighbor azimuthal approach will both ignore small-scale features and represents the elongation of the MVF outline (Le Corvec et al. 2013). This is a problem because any eruptive center is likely more related to its nearest neighbors than further neighbors (Cebriá et al., 2011). For this reason, a method of eliminating insignificant data must be derived. Based on the fact that any eruptive center is likely most related to its nearest neighbors, we choose to filter the azimuths based on length. Meaningful azimuths are ones in which the constituent vents have a high probability of being related. Cebriá et al. (2011) found that the optimum cutoff length is one-third of the mean azimuth length,  $\mu$ , minus the standard deviation  $\sigma$ .

$$d_{crit} \le \frac{\mu - \sigma}{3}$$

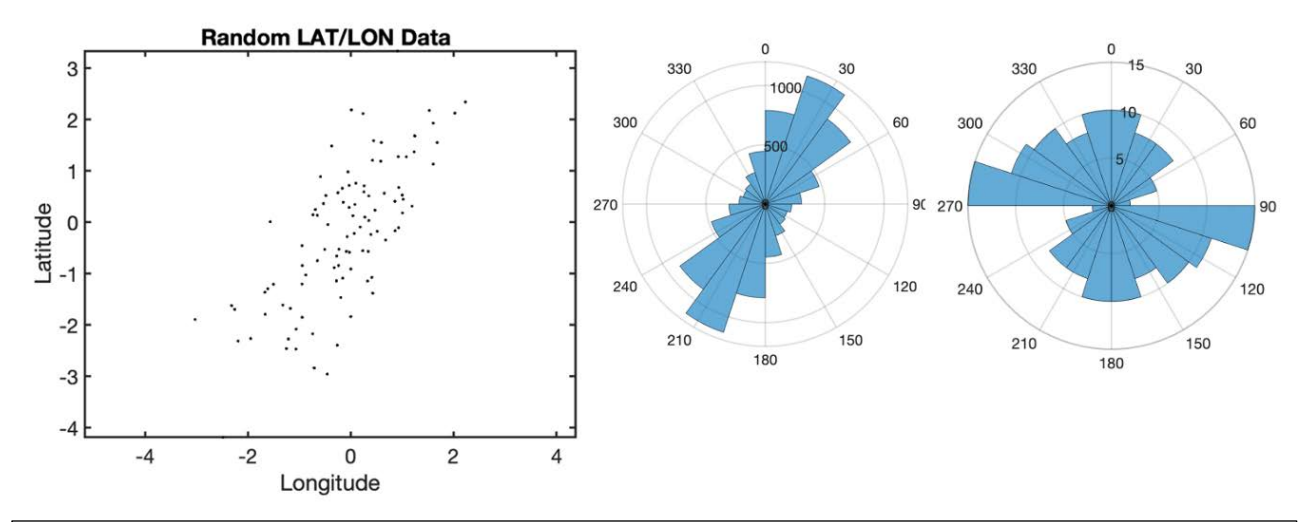


Figure 12

The scatter plot to the left is of randomly generated vent data centered on y = x. The leftmost rose diagram is an unfiltered representation of all azimuths within the dataset. The rightmost rose diagram is filtered by  $d_{crit}$ .

An array containing the azimuth data corresponding to the pairs of points with distance between them less than  $d_{crit}$  is built in MATLAB. This array will only contain the forward azimuths. To see both the forward and back-azimuths in the rose diagram, both  $A_m$  and  $A_m + \pi$  are plotted simultaneously: this plot will be radially symmetric. If the plot is uniformly distributed, there is no preferred orientation of the alignments. Drawing the meaningful azimuths onto the original scatter plot with vent locations begins to reveal spatial patterns in the distribution. Clusters, alignments, and gaps become more apparent. A preferential alignment will be more apparent once azimuths between further separated vents are eliminated. This criterion allows only the azimuths collected over the shortest distance to be considered. For fields with a large number of vent-pairs ( $N \ge \sim 100$ ),  $d_{crit}$  will be significantly shorter than the length of the most elongated axis of the field, effectively eliminating the influence of the field's overall geometry on the predominant strike. These azimuths can be drawn onto a scatter plot for visual interpretation as in Figure 12.

### 4.2 Determining the significance of alignment

Calculating the significance of the vent alignments is an important step in determining whether there is a relationship between vent distribution and the stress field. In order to calculate the agreement between the mean azimuth and the most compressive stress direction, there must be a statistically significant mode amongst the azimuths. There are two methods listed in the Circular Statistics toolbox by Berens—the Omnibus Test and the Rayleigh Tests for uniformity. The Omnibus test holds less power than the Rayleigh Test, but the Rayleigh Test is only applicable to Von Mises distributions of which the distribution of vent-to-vent azimuths is not. The Omnibus Test for circular uniformity is an alternative to the Rayleigh test that works well for unimodal, biomodal and multi-modal distributions and does not make specific assumptions about the underlying distribution (Berens, 2009). For this reason, the Omnibus Test for uniformity is used in this study. The test statistic, *P*, is calculated as:

$$P = \frac{1}{2^{N-1}}(N-2m) \binom{N}{m}$$

The null hypothesis of this test is that the dataset is uniformly distributed around the unit circle. In geologic terms, this would mean that there is no preferred orientation of the significant vent-to-vent azimuths within the MVF. Conversely, the alternative hypothesis is that there are a preferred azimuth orientation and a significant mode. In MATLAB, this test will return a p value. If p < a selected  $p_{crit}$ , the null hypothesis,  $H_0$  can be rejected (Figure 13).

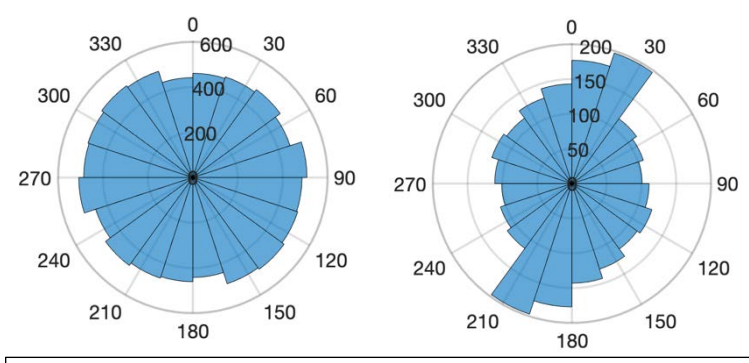


Figure 13

The leftmost histogram is of azimuths between randomly generated vents—Omnibus test returns p=0.18. The rightmost histogram is from the Newberry MVF—The omnibus test returns p=0.0001.

#### 4.3 Comparison to Stress Environment

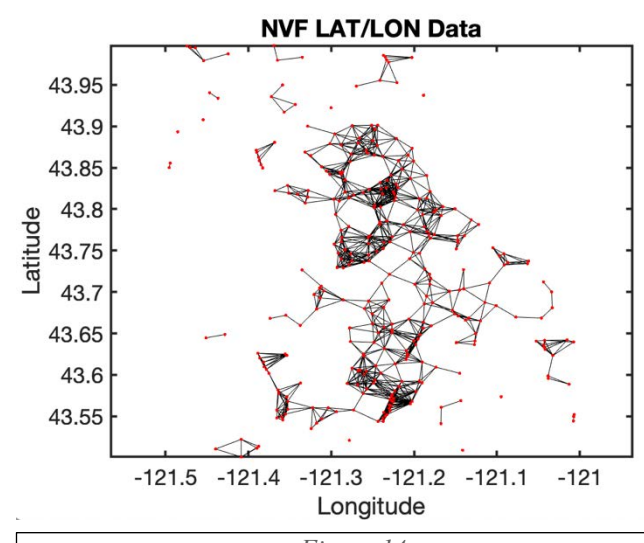
Beyond visual interpretation, there are rigorous mathematical methods of quantifying the agreement of the mean azimuth and the direction normal to the least compressive stress direction—one of which is the V-Test for uniformity (Landler et al., 2018; Berens, 2009). The test statistic, V, is computed as:

$$V = R_n \cos(\bar{\alpha} - \bar{\alpha}_A)$$

This test takes a distribution of circular data and compares the distribution to a proposed mean direction. The circular V-Test has an alternate hypothesis  $H_A$  that the distribution is not uniform and has a mean direction consistent with a predetermined mean (Berens, 2009). The null hypothesis  $H_0$  states either that the distribution is uniform or that the selected predetermined mean is inconsistent with the distribution (Berens, 2009). The predetermined mean input can effectively be replaced with the direction normal to the least principal stress since it is hypothesized that the predominant alignment of the MVF is parallel to the most compressive stress. The V-Test will return a p-value that can be compared to a critical p value,  $p_{\text{crit}}$ . If  $p < p_{\text{crit}}$ , the null hypothesis,  $H_0$  can be rejected. Reasonable values for  $p_{\text{crit}}$  depend on desired tolerance. For example, if an analysis requires 95% confidence in a result,  $p_{\text{crit}} = 0.05$  would be chosen. For the example given, an arbitrary most compressive stress oriented at 270° is tested. The V-Test returns a p of 0.5. This is a large p-value which means there is only a 50% chance that  $H_a$  is true. In this case the null hypothesis is accepted, even though the mean azimuth of the dataset at 8° is near to the direction of the most compressive stress running N-S This is an expected result considering the dataset is completely random, is relatively uniform, and has a large dispersion.

### 5 Results

### 5.1 Newberry Volcanic Complex Results



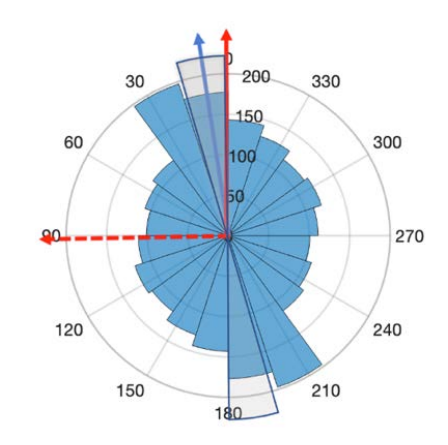


Figure 14

Newberry MVF Vent locations with azimuths drawn.

Figure 15

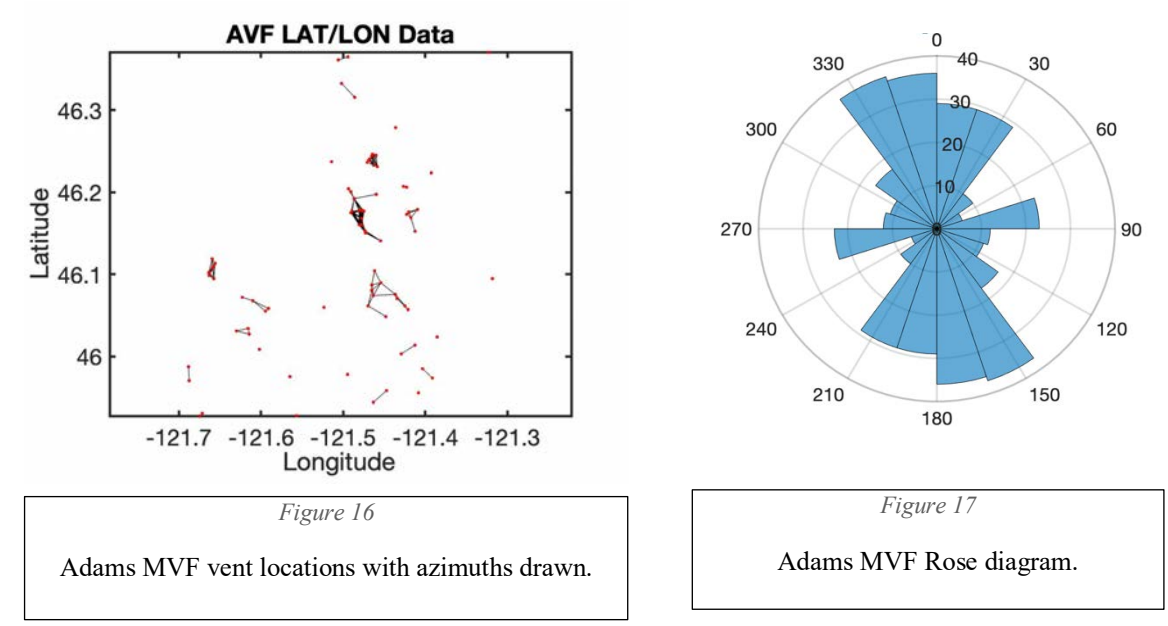
The most compressive stress direction is indicated in red; the average azimuth with 5% error bars is in blue.

The significant azimuths of the Newberry MVF can be seen in Figure 14. By inspection of the rose diagram in Figure 15, most azimuths of the Newberry Volcanic Field are aligned roughly N-S. This is confirmed by the rose diagram. It is clear that there is a mode between 0° and 45°. Visually, the mode is strong enough that the data are not uniformly distributed and are diametrically bimodal. The V-test can be used to evaluate the agreement between the mean azimuth and the most compressive stress. The most compressive stress for this region was calculated by averaging the stress orientations surrounding the Newberry MVF taken from the WSM. The two closest stress measurements (within ~1° of latitude or longitude) to the North of the field were averaged returning a most compressive stress of 1°. The WSM has these stress measurements listed as generated from focal mechanisms from a thrust faulting stress regime.

	Latitude (degrees)	Longitude (degrees)	Strike of MCS (degrees)	Quality
a.	45.154°	-120.861°	5°	C
b.	45.220°	-120.770°	357°	С

A visualization of the most compressive stress overlaying the azimuths can be seen in Figure 15. The Omnibus test returns  $p \approx 0.001$ . The V-test comparing the Newberry vent-location data and the most compressive stress at 1° returned a p of 0.030 which means there is a 3% chance that the most compressive stress is not significantly parallel to the mean azimuth. At a standard confidence tolerance of  $p_{crit} = 0.050$ , the alternative hypothesis that the most compressive stress direction is parallel to the predominant alignment of this MVF can be accepted for the Newberry MVF.

#### 5.2 Adams Volcanic Field Results



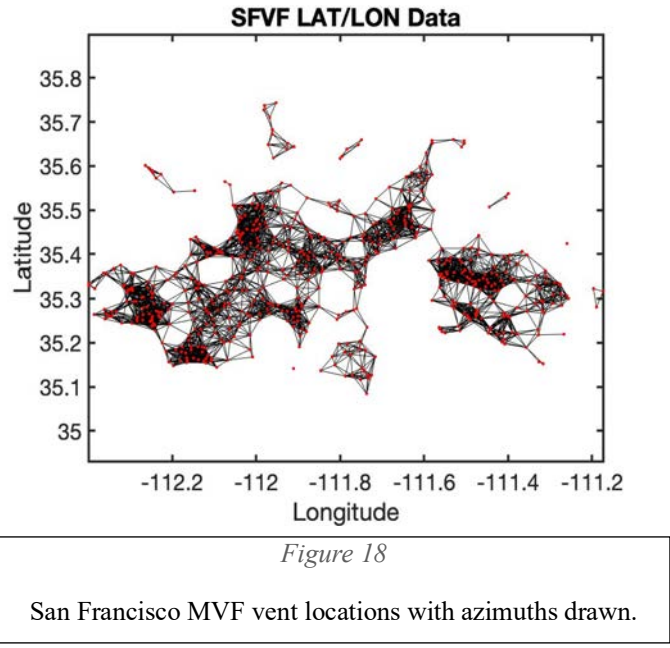
The stress field is very well-documented for the Adams Volcanic Field. This is likely due to Mount Adams' proximity a subduction zone where there are more earthquakes. There are nearly 100 stress measurements within  $\pm$  1° of latitude or longitude to the central edifice, Mount Adams; However, to constrain the scope of the stress data, only stress measurements from latitude 46° to 47° and longitude -122° to -121° will be used. These are the approximate bounds of the vent location data used in the project, so only stress measured within the field are used. There are 13 independent stress measurements in this range—each of which is measured from focal mechanisms and is of quality grade C. The circular mean of the most compressive stress is oriented at -1° with a circular standard deviation of  $\pm$  11°, showing a good consistency between these estimates. Considering a proper population standard deviation is calculated with at least 20-25 measurements, a spread of  $\pm$ 11° is promisingly small. This leads me to believe that the stress direction of -1° is well-defined and that the regional most compressive stress is oriented approximately N-S.

	Latitude (degrees)	Longitude (Degrees)	Strike of MCS (Degrees)	Quality
a.	46.760	-121.520	167	C
b.	46.529	-121.389	13	C
c.	46.528	-121.385	175	С
d.	46.521	-121.376	8	C
e.	46.530	-121.399	5	C
f.	46.970	-121.940	165	C
g.	46.570	-121.840	16	C
h.	46.525	-121.394	10	C
i.	46.540	-121.450	174	С
j.	46.822	-121.831	174	С
k.	46.791	-121.520	170	С
1.	46.679	-121.333	162	С
m.	46.546	-121.378	7	С

There is a distinct mode of the azimuths of the Adams Volcanic Field vent alignments (Figure 16; Figure 17); The Omnibus Test returns a p value of  $1.7 \times 10^{-8}$ . This confirms that there is a very strong preferred alignment of vents. From the average of the azimuths in the Adams MVF, the vent alignment within the field is oriented at -6°. Comparing the average azimuth of -6° and the most compressive stress direction, the V-test returns  $p = 3 \times 10^{-11}$  which indicates that

there is a very strong relationship between the preferred orientation of volcanic vent alignments and the regional stress field.

#### 5.3 San Francisco Volcanic Field Results



The San Francisco Volcanic Field is a much more challenging field to analyze considering the nature of the stress directions from the WSM. The stress map of the San Francisco MVF shows two approximately orthogonal stress directions within the field, one at 37° by averaging measurements circled in red in Figure 16 below, and the other at 134° circled in orange. All three utilized measurements from the WSM are determined by earthquake focal mechanisms. Note that are other stress measurements within the field which are determined by vent alignments. In order to limit bias, these measurements are omitted because estimates of stress from vent alignments are not independent of the vent alignments calculated in this study.

	Latitude (degrees)	Longitude (degrees)	Strike of MCS (degrees)	Quality
a.	35.160°	-112.250°	44°	С

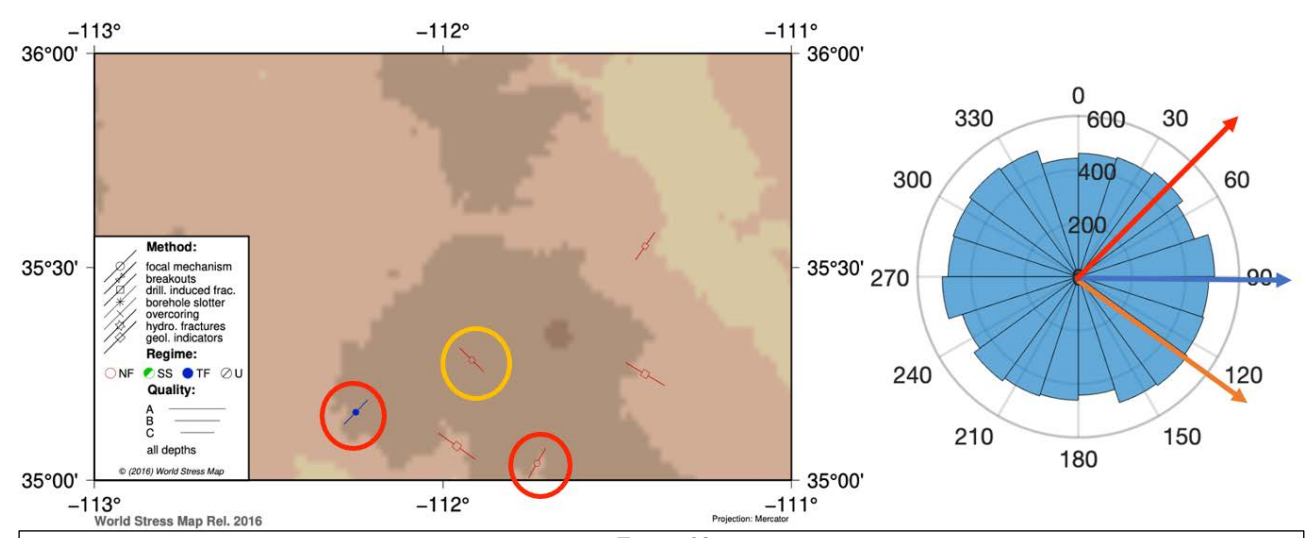


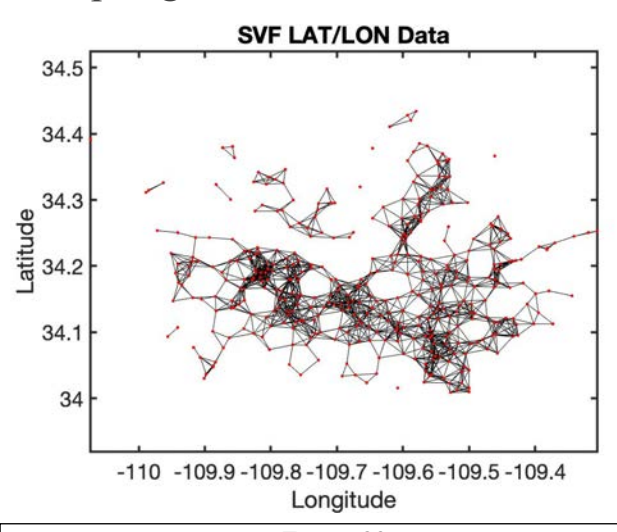
Figure 19

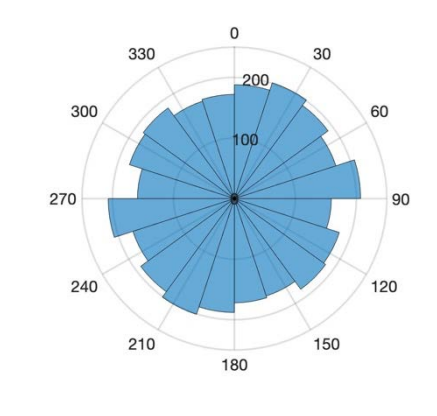
The SFVF has two approximately orthogonal stress directions: one circled in red (37°) and the other circled in orange (134°). These directions are overlayed on the rose diagram to the right.

b.	35.283°	-111.917°	134°	С
c.	35.040°	-111.730°	30	C

The field in general appears very uniform (Figure 19)—this is supported by the Omnibus Test for uniformity which returns a p of 0.17. Although insignificant, the mean azimuth of the field is 91°. Comparing the mean azimuth with the two proposed stress directions, 37° and 134°, the V-test returns p = 0.88, 0.16 respectively. The p values between the average azimuth and both proposed stress directions. Based on the p values for the Omnibus Test and for the V-test compared to p, it can be safely assumed that the vent alignments of the San Francisco MVF are statistically not parallel to the most compressive local stress.

### 5.4 Springerville Volcanic Field Results



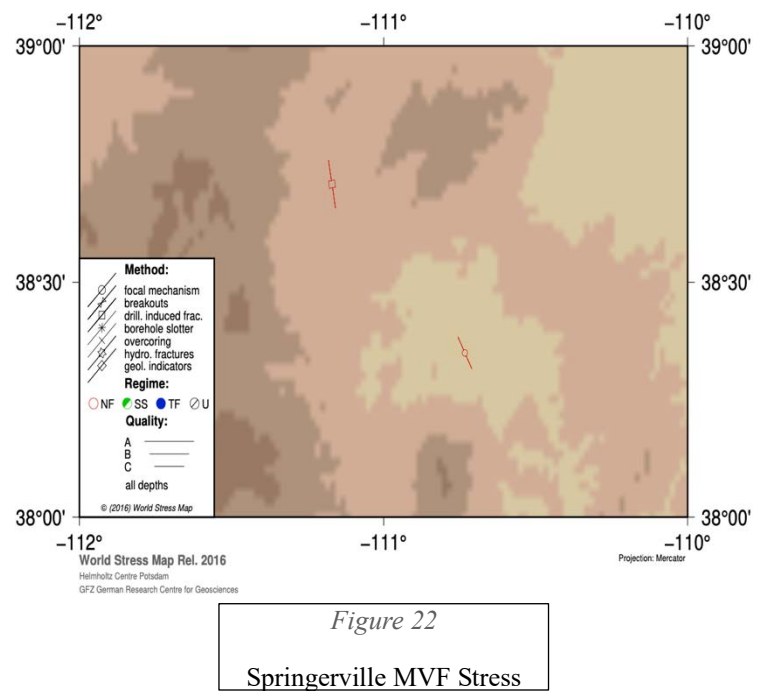


 $\label{eq:Figure 20} Figure \ 20$  Springerville MVF vent locations with azimuths drawn.

Figure 21
Springerville MVF rose diagram.

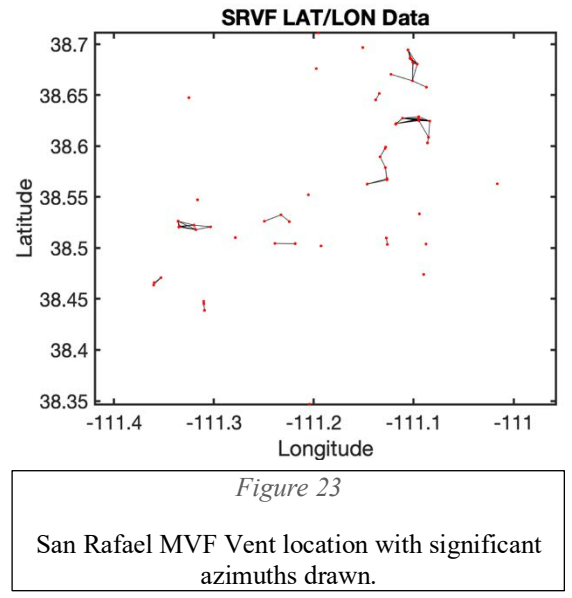
The Springerville Volcanic Field is much like the San Francisco Volcanic Field in terms of stress measurements. There are two approximately orthogonal most compressive stress measurements—one at 8° and another at 104° as seen in Figure 22. Note that the WSM only has stress estimates derived from vent alignments within the scope of Springerville MVF, so there is some intrinsic bias included in the analysis of this field.

		Latitude (degrees)	Longitude (degrees)	Strike of MCS (degrees)	Quality
г	ì.	34.23°	-109.630°	8°	C
ŀ	٥.	34.140°	-109.680°	105°	A



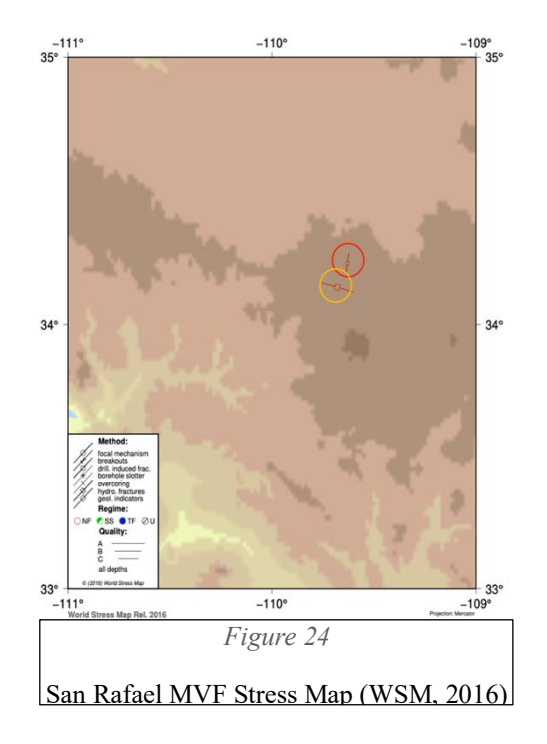
The Springerville Volcanic Field appears extremely uniform (Figure 20; Figure 21). This is confirmed by the Omnibus Test which returns p=0.065. At a  $p_{crit}$  of 0.05, we accept the null hypothesis that there is no preferred orientation of azimuths. The mean azimuth of 88° is insignificant. The V-test returns p=0.70, 0.14 for stress directions of 8°, 104° respectively. Note that the measurement with a strike of 105° is of quality A which should be given more power. Based on a  $p_{crit}$  of 0.05, we can accept the null hypotheses that there is no preferred orientation of vent alignments and that the mean azimuth is not parallel to the most compressive stress.

#### 5.5 San Rafael Volcanic Field Results



There is only one stress measurement from the WSM that applies to the San Rafael Volcanic Field — the strike is oriented at 152° and was calculated by using an earthquake focal mechanism. The other stress measurement listed by the WSM that was estimated by vent alignment and is omitted as it would not be independent of the analysis done here (Figure 24; Figure 25).

	Latitude (degrees)	Longitude (degrees)	Strike of MCS (degrees)	Quality
a.	38.350°	-110.733°	152°	C



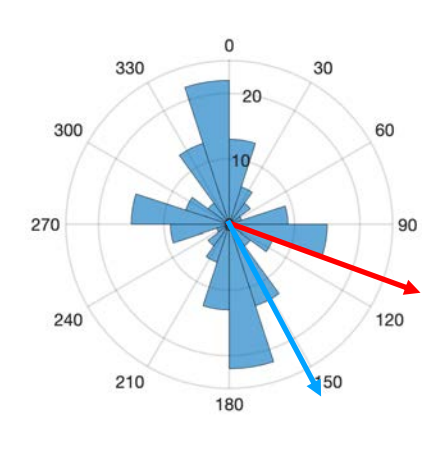


Figure 25
San Rafael MVF Rose diagram

The san Rafael Volcanic field is different from the other fields covered so far. There are two distinct modes, one major and one minor, when observing a circular histogram. The Omnibus test returns a p of 0.018 meaning the azimuths within the San Rafael MVF have a preferred orientation. The V-test returns a p value of 0.98. Although the field has a statistically significant vent alignment, there is no significant correlation between the mean azimuth of 110° and the most compressive stress direction. The rose diagram, however, makes it clear that the secondary mode of azimuth in the San Rafael MVF is very close to the most compressive stress direction.

### 6 Discussion

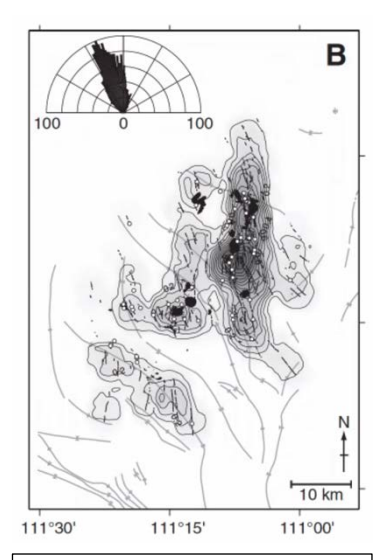
### 6.1 Regional vs. Local Stress

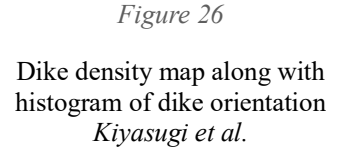
The regional stress field appears to have a much larger effect on vent alignments within an MVF than the local stress field. The presence of a central vent within an MVF may also have a positive impact on vent alignments correlating to the stress field. The two fields with a central vent—again Newberry and Adams—have vent distributions seemingly dependent on the orientation of the regional stress field.

At the Spanish Peaks, the dikes propagate radially according to the local stress field. Its only later that the regional stress takes control of their orientation. Perhaps the regional stress has a larger effect on conduit propagation where the local stress has a larger effect on dike propagation. The local stress field seems to have very little negative effect on vent alignment within distributed fields, or at least a much smaller effect than the regional stress. In fact, only the fields with a central edifice had any correlation between vent-to-vent azimuths and the most compressive stress. This may be due to differing levels of stress between the local and regional stress fields. The regional stress along a convergent boundary like the Juan de Fuca Subduction Zone may be much larger than the local stress created by a central vent like Newberry or Mount Adams. There also may be a correlation between tectonic environment and the presence of a central vent in an MVF, but the scope of this project is too small to make any conclusions on that postulation.

#### 6.2 San Rafael

Kiyosugi et al. (2012) studied the density of dikes at the San Rafael Swell. Their rose diagram of dike orientation features a major mode at 165°. The mode of that histogram appears to match almost perfectly to the major mode of azimuths between the nearest vents of the field. Furthermore, the minor mode of the azimuths found in my study appears to correspond well with the most compressive regional stress from WSM. The two modes of the San Rafael MVF could correspond to different populations, perhaps distinct in time. As the stress field is measured from present day, the minor mode may correspond to younger dikes, and the major mode to older dikes that may have been influenced by a different, earlier stress field. There also may be a





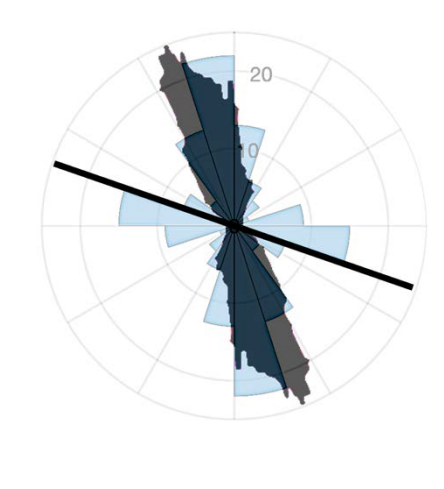


Figure 27

San Rafael MVF Rose diagram with dike orientation diagram and most compressive stress overlayed.

preexisting fabric in the minor mode direction. The azimuths of the major mode dikes could follow the present stress field while the major mode dikes may simply reuse preexisting structures from an older stress regime.

#### 6.3 Tectonic Environment

The Adams and Newberry Volcanic fields are located in proximity to the Juan De Fuca Subduction Zone. The fact that MVFs near subduction zones have defined alignments that correlate well to the regional stress field may imply that stress is larger at convergent boundaries. This may seem intuitive, but it is actually a debated topic whether or not the stress is larger at subduction zones or if the material is weaker, which would lead to lower stress. The correspondence between MCS and vent alignment at these subduction zone volcanoes may provide evidence that the stress related to the Juan de Fuca subduction zones is indeed larger than in an intraplate setting. This would make sense because in order to overpower the local stress felt at these fields with a central vent, there must be a rather large regional stress—especially because there is such a good agreement between the most compressive stress and alignment at Newberry and Adams.

### 7 Conclusion

The regional stress field seems to have a large effect on vent distribution in some monogenetic volcanic fields. It was found that for vent fields located above a subducting plate—Newberry Volcanic Complex and Adams Volcanic Field—there is not only a statistically significant mode of vent-to-vent azimuths, but that mode also significantly correlates to independent stress measurements from the World Stress Map. This may be due to a higher compressive stress components around convergent boundaries, although this is a debated idea.

Though not based in data analysis, there seems to be some sort of agreement between the orientations of the dikes in the San Rafael volcanic field and the preferred alignment of conduits found by my analysis. Based on data from Kiyosugi et al., 2012, the mode of dike orientations within the San Rafael MVF appears to match well with the major mode of the rose diagram of azimuths from the field. The secondary mode of the rose diagram for the San Rafael MVF appears to have a relationship to the current most compressive stress from WSM. This leads me to believe

age of vents may have an effect on agreement between stress and vent alignment and the field of the San Rafael MVF has rotated over time.	at the stress

#### 8 Works Cited

- Berens, P. (2009). CircStat: A MATLAB Toolbox for Circular Statistics. *Journal of Statistical Software*, 31(10).
- Carlson, R. W.; Grove, T. L.; Donnelly-Nolan, J. M. (April 2018). "Origin of primitive tholeiitic and calc-alkaline basalts at Newberry Volcano, Oregon". *Geochemistry, Geophysics, Geosystems.* **19** (4): 1360–1377.
- Cebriá, J., Martín-Escorza, C., López-Ruiz, J., Morán-Zenteno, D., & Martiny, B. (2011). Numerical recognition of alignments in monogenetic volcanic areas: Examples from the Michoacán-Guanajuato Volcanic Field in Mexico and Calatrava in Spain. *Journal of Volcanology and Geothermal Research*, 201(1-4), 73-82.
- Condit, C. D.; C. B. Connor (October 1996). "Recurrence rates of volcanism in basaltic volcanic fields; an example from the Springerville volcanic field, Arizona". *GSA Bulletin*. Geological Society of America. **108**. Retrieved 2009-01-13.
- Connor, C. B., Connor, L., Germa, A., Richardson, J., Bebbington, M., Gallant, E., & Saballos, A. (2019). How to use kernel density estimation as a diagnostic and forecasting tool for distributed volcanic vents. *Statistics in Volcanology*, 4, 1-25.
- Corvec, N. L., Spörli, K. B., Rowland, J., & Lindsay, J. (2013). Spatial distribution and alignments of volcanic centers: Clues to the formation of monogenetic volcanic fields. *Earth-Science Reviews*, 124, 96-114.
- Donnelly-Nolan, J. M.; Stovall, W. K.; Ramsey, D. W.; Ewert, J. W.; Jensen, R. A. (2011). Hendley II, J. W. (ed.). *Newberry Volcano Central Oregon's Sleeping Giant: USGS Fact Sheet 2011–3145* (PDF). United States Geological Survey.
- Fillmore, Robert (2011). Geological Evolution of the Colorado Plateau of Eastern Utah and Western Colorado. University of Utah Press. <u>ISBN</u> 978-1-60781-004-9.
- Foshag, W.P., and G.R. Gonzales (1956). Birth and development of Paricutin volcano, Mexico. U.S. Geol. Surv. Bull. 965-D, 355-489. DOI: 10.3133/b965d
- Johnson, R. B. (1968), Geology of the igneous rocks of the Spanish Peaks region, Colorado, Geol. Soc. America Bull. 47, 1727–1784.
- Kienle, J.; Wood, C. A., eds. (1992). *Volcanoes of North America: United States and Canada*. Cambridge University Press. ISBN 978-0-521-43811-7.
- Kiyosugi, K., Connor, C. B., Wetmore, P. H., Ferwerda, B. P., Germa, A. M., Connor, L. J., & Hintz, A. R. (2012). Relationship between dike and VOLCANIC CONDUIT distribution in a highly ERODED monogenetic volcanic Field: San Rafael, Utah, USA. *Geology*, 40(8), 695-698. doi:10.1130/g33074.1
- Luhr J F, and T. Simkin (1993). Paricutin: The Volcano Born in a Mexican Cornfield. Phoenix: Geoscience Press, 427 p.

- ODÉ, H. (1957). MECHANICAL analysis of the dike pattern of the Spanish Peaks area, colorado. *Geological Society of America Bulletin, 68*(5), 567. doi:10.1130/0016-7606(1957)68[567:maotdp]2.0.co;2
- Robinson, J. E., Donnelly-Nolan, J. M., & Jensen, R. A. (2015). Newberry Volcano's youngest lava flows. Scientific Investigations Map. US Geological Survey. https://doi.org/10.3133/sim3329
- Valentine, G., & Gregg, T. (2008). Continental basaltic volcanoes Processes and problems. *Journal of Volcanology and Geothermal Research*, 177(4), 423-434.
- Wadge, G., & Cross, A. (1988). Quantitative methods for detecting aligned points: An application to the volcanic vents of the Michoacan-Guanajuato volcanic field, Mexico. *Geology*, 16(9), 815.
- Walker, G. W. (July 1974). "Some implications of late Cenozoic volocanism to geothermal potential in the High Lava Plains of south-central Oregon" (PDF). Ore Bin. Open-File Report. 36 (7): 109–119.

# 9 MATLAB Script (Original)

#### Datasets available by request

```
function ventanalysis(ventsetFile, ventName, stressdir)
%% MAKE UP DATASET;
% calculate automatically vent field statistics and evaluate a few
% directions
% ventsetfFile: data file .xy
% ventName: shorthand for vent field
% stressdir:
               direction to test
% example used:
%
  ventanalysis('svf.vents.ll.xy','SVF',90)
%
  ventanalysis('adams.vents.ll.xy','AVF',0)
  ventanalysis('newb.vents.ll.xy','NVF',7)
%
   ventanalysis('sanraf.vents.ll.xy','SRVF',90) (Green River)
   ventanalysis('SFVF_allvents_longlat.xy','SFVF',90) (near Flagstaff)
           B = Brunhes, ventanalysis('B_vents_longlat.xy', 'SFVF', 90)
           M = Matuyana, ventanalysis('M_vents_longlat.xy','SFVF',90)
           P = Pre-Mat, ventanalysis('P_vents_longlat.xy','SFVF',90)
%
%% LOAD VENTS
ventset = load(ventsetFile, 'ascii')
X = ventset(:,1);
Y = ventset(:,2);
%% RANDOM DATASETS (Use any field)
% X = randn(100,1); % use for random dataset
% Y = randn(size(X)); % use for random Y dataset
% Y = X + randn(100,1); % use for random dataset centered on x = y (demonstrates
d crit's effect)
nx = length(X);
%% DEFINE AZIMUTHS
% point-to-point distance and azimuth
Xa=repmat(X,[1,nx]);
Ya=repmat(Y,[1,nx]);
[Dm, Am] = distance(Ya, Xa, Ya', Xa', 'degrees');
D=squareform(Dm);
%% D_CRIT
% select pairs separated by less than a critical distance
limit = ((sum(D)/((nx*(nx-1))/2))-std(D))/3;
Du=triu(Dm); Du(find(Du==0))=NaN;
[row,col]=ind2sub(size(Du),find(Du<limit));</pre>
%% MAKE THE PLOTS
ventTitle=sprintf('%s LAT/LON Data', ventName);
% Vent Map
figure (1); clf, box on; hold on;
scatter(X,Y,'black','.'); axis equal; box on; title(ventTitle); xlabel
'Longitude'; ylabel 'Latitude'
set(gca,'linewidth',2,'fontsize',18)
hold off
% W/ Drawn Azimuths
figure(2); clf; axis equal; box on; hold on;
plot([X(row),X(col)]',[Y(row),Y(col)]','black')
scatter(X,Y,'red','.'); title(ventTitle); xlabel 'Longitude'; ylabel 'Latitude'
```

```
set(gca, 'linewidth', 2, 'fontsize', 18)
hold off
% Rose Diagram
figure(3); clf
Azis = deg2rad(mod(Am(sub2ind(size(Am),row,col)),180))
polarhistogram([Azis Azis+pi],20)
set(gca,'ThetaZeroLocation','top')
set(gca,'linewidth',2,'fontsize',18)
set(gca,'Thetadir','clockwise')
thetalim([0 360])
hold off
%% SET MEAN AND LCSD
MCS = (stressdir)
MCS2 = (104)
mean = rad2deg(circ_mean(2*Azis)/2)
stdev = rad2deg(circ_std(2*Azis)/2)
%% TESTS OF UNIFORMITY
% Rayleigh Test
p crit = 0.05
[pval_r, z_r] = circ_rtest(2*Azis)
if pval_r < p_crit</pre>
    fprintf('field passes Rayleigh test')
else
     disp('field fails Rayleigh test')
end
% Omnibus Test
[pval_o, z_o] = circ_otest(2*Azis)
if pval_o < p_crit</pre>
     disp('field passes Omnibus test')
else
     disp('field fails Omnibus test')
end
disp(' ')
%% TEST DATASET AGAINST STRESS DATA
% Defining Angles
allAngles=[MCS, MCS2, mean]; % common angles
nAngles=numel(allAngles);
pval=NaN(size(allAngles));
v=NaN(size(allAngles));
u = cos(deg2rad(allAngles));
v = sin(deg2rad(allAngles));
for iA=1:nAngles
    [pval(iA), v(iA)] = circ_vtest(Azis, allAngles(iA));
end
disp(sprintf('for A=%g, p=%g\n',[allAngles;pval]));
print(1,'-dpdf',sprintf('%s.ventMap.pdf',ventName));
```